

# Transducer to Transducer Time Domain Signal Response Shaping in Ultrasonic Applications

Jean-Paul Sandoz

Electrical Engineering Department

HE-ARC / HES-SO

Le Locle, Switzerland

e-mail: jean-paul.sandoz@he-arc.ch

**Abstract**— This paper presents the investigation of a new solution whose purpose is to obtain a much shorter time domain response between two narrow-band transducers than the one which is produced by a short reference driving pulse (SRP). It is based on generating a new driving signal made up of an appropriate weighted series of SRP which will produce the desired objective time response (OTR). Concretely, the SRP time response of our targeted application is determined and the OTR is selected from it. Finally, the minimum mean square error (MMSE) criterion is applied to compute the weights of the new driving signal. Complete series of practical tests with different kinds of transducers operating in varied conditions have confirmed the theoretical results.

**Keywords:** Time Domain Response Shaping; Minimum Mean Square Error; Weighted Series of Pulses

## I. INTRODUCTION

In many ultrasonic applications, the transducer to transducer time domain signal response is critical for precise and reliable measurement of physical properties or specific process parameters estimations [1]. While the signal-to-noise ratio will often limit the achievable system performances, several techniques having being successfully used for its enhancement (e.g., [2]). However, in situations where narrow pulses have to be used as driving signals, the interaction of ultrasonic transducers with their environment will often produce time domain responses (TDR) which are far too long for the targeted application. Whereas the classical solutions to this problem involve the use of heavy mechanical dumping with its inherent loss of sensitivity, we solve this difficulty with an innovative approach which is exclusively based on digital signal processing techniques.

From signal processing theory (e.g., [3] and [4]), it is theoretically possible to find an input signal to a linear transfer function that will produce almost any TDR. Thus, the challenge was to find a robust way to create a new driving signal able to significantly reduce the TDR duration. Moreover, in order to make easy a practical implementation, this signal was chosen in the form of a weighted series of short identical duration reference pulses. Since in many ultrasonic applications the real signals have inevitably some embedded complexity (e.g. multi resonances), we used a technique based on the MMSE criterion.

This paper is organized as follows: The basic theoretical analysis of the proposed solution is given in section 2. Next, complete practical examples are presented. Finally, the last section summarizes the advantages of this design and suggests potential developments along with application domains that can benefit from this original solution.

## II. THEORETICAL ANALYSIS

### A. Basic Block Diagram

The basic block diagram is given in Fig. 1 where:

$x(t)$  : Driving signal

$h_T(t)$  : Transmitter transducer impulse response

$h_C(t)$  : Transmission channel impulse response  
(dispersive or non-dispersive)

$h_R(t)$  : Receiver transducer impulse response

$y(t)$  : Global system response to  $x(t)$  excitation

Assuming linearity and time invariance, then:

$$y_{SRP}(t) = x_{SRP}(t) * h_T(t) * h_C(t) * h_R(t) \quad (1)$$

where  $*$  denotes the convolution operator and

$x_{SRP}(t)$ : Short reference driving pulse

$y_{SRP}(t)$ : Short reference driving pulse global system response

All these definitions can be rewritten in the discrete time domain. Thus

$$y_{SRP}(n) = x_{SRP}(n) * h_T(n) * h_C(n) * h_R(n) \quad (2)$$

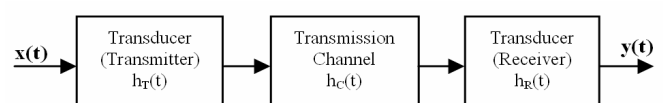


Figure 1. Basic block diagram

**B. Global System Response Shaping**

Let:

$$x_{MPL}(n) = a_0 \cdot x_{SRP}(n) + a_1 \cdot x_{SRP}(n-1) + a_2 \cdot x_{SRP}(n-2) + \dots$$

$$\text{or: } x_{MPL}(n) = \sum_{k=0}^{N-1} a_k \cdot x_{SRP}(n-k) \quad (3)$$

$x_{MPL}(n)$  is a **weighted series of  $N$  short reference pulses**.

The superposition principle implies

$$x_{SRP}(n) \rightarrow y_{SRP}(n) = p(n)$$

$$x_{MPL}(n) \rightarrow y_{MPL}(n) = Mp(n)$$

and is equivalent to

$$Mp(n) = \sum_{k=0}^{N-1} a_k \cdot p(n-k) \quad (4)$$

corresponding to the **multiple pulses response system**.

**C. MMSE Criterion**

At this point, the desired OTR is chosen from the short reference driving pulse global system response, i.e.  $Mobj(n)$ . Then, from the MMSE criterion, the  $N$  weights  $a_k$  of the new driving signal must satisfy the following relationship:

$$\varepsilon(a_k)_{\text{minimum}} = \left[ \sum_{n=\min}^{\max} ((Mp(n) - Mobj(n))^2) \right]_{\text{minimum}} \quad (5)$$

$\min$  and  $\max$  define the bounds between which the MMSE algorithm will be applied.

**D. Theoretical Solution**

From linear algebra

$$\frac{d}{da_k} \varepsilon(a_k) = 0 = \frac{d}{da_k} \sum_{n=\min}^{\max} ((Mp(n) - Mobj(n))^2) \quad (6)$$

Equation (6) generates a set of  $N$  linear equations with the following solution:

$$A = Rpo^T Rpp^{-1} \quad (7)$$

where

$$Rpo_k = \frac{1}{\max - \min} \cdot \sum_{n=\min}^{\max} Mobj(n) \cdot p(n-k) \quad (8)$$

$$Rpp_{k,l} = \frac{1}{\max - \min} \cdot \sum_{n=\min}^{\max} p(n-k) \cdot p(n-l) \quad (9)$$

$Rpo$  = SRP-OTR cross-correlation vector

$Rpp$  = SRP auto-correlation matrix

$k = 0 \dots N-1, \quad l = 0 \dots N-1$

$A = [a_0, a_1, a_2 \dots a_{N-1}]$

Therefore, the MMSE criterion implies that the weights of the new driving signal are given by the product of the SRP-OTR cross-correlation vector with the inverse SRP auto-correlation matrix.

**III. PRACTICAL EXAMPLES**

In order to demonstrate the performances of the proposed solution, the next two practical examples are drawn from a representative selection of real situations.

**A. 40 kHz Ultrasonic Air-Transducers**

In this example, a pair of popular low cost 40 kHz air transducers is considered. The set-up shown on Fig. 2 was used to first determine the transducer to transducer short reference driving pulse response  $p(n)$ . A sampling rate of 312.5 kHz was selected with one sample interval (3200 ns) as the driving pulse width duration. In this signal acquisition, it is very important to make sure that no reflections or multi-path signals get mixed-up with the direct wave; therefore the two transducers holders (white wooden frames) are not parallel to one another. The signal  $p(n)$  is shown on Fig. 3. The initial delay is due to the global propagation time (i.e. air + transducers).



Figure 2. Experimental set-up: Two 40 kHz air-transducers, one arbitrary waveform generator (ETC M631), one PC oscilloscope (PicoScope® 3223)

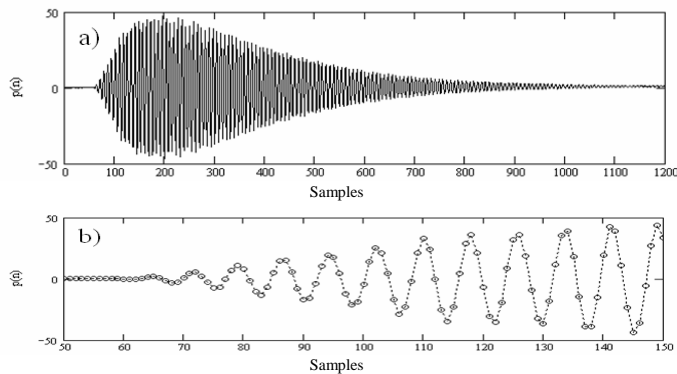


Figure 3. Samples of  $p(n)$  a)  $0 \rightarrow 1200$ , b)  $50 \rightarrow 150$

Assuming 8 samples per cycle,  $p(n)$  goes on more than 50 cycles. Next, a preliminary objective response  $Mpre(n)$  is picked out from a time delayed version of  $p(n)$ . Then,  $Mobj(n)$  is computed as follows:

$$Mobj(n) = Mpre(n) W(n) \quad (10)$$

where  $W(n)$  is a windowing function. All these different steps are depicted on Fig. 4.

Subsequently, the weights are computed and displayed on Fig. 5, whereas Fig. 6 presents an overlay of  $Mobj(n)$  and  $Mp(n)$ . In this example we chose  $N = 200$ .

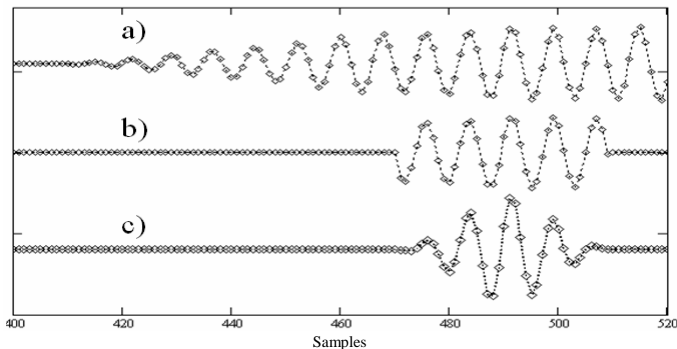


Figure 4. a)  $p(n-350)$ , b)  $Mpre(n)$  and c)  $Mobj(n)$

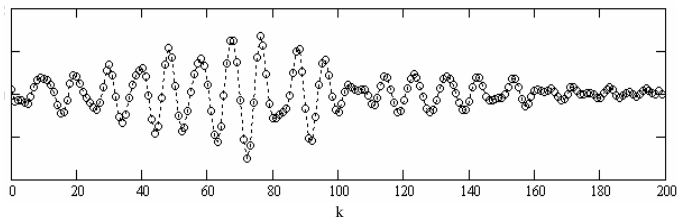


Figure 5. Weights  $a_k$

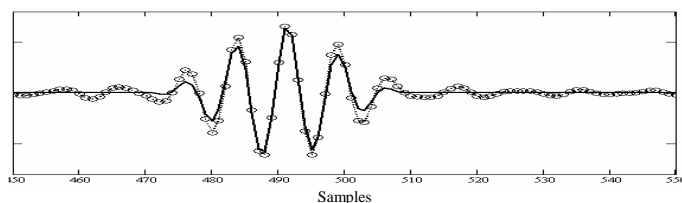


Figure 6. Continuous line:  $Mobj(n)$ , Circles:  $Mp(n)$

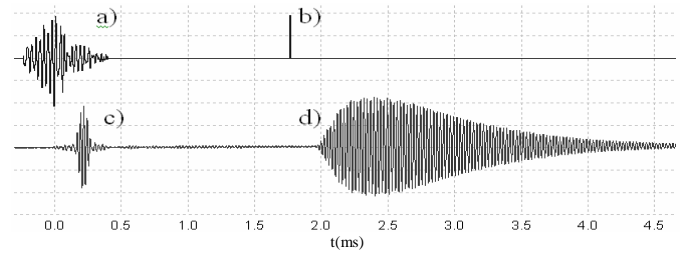


Figure 7. a)  $x_{MPL}(t)$ , b)  $x_{SRP}(t)$ , c)  $M_{p\text{practical}}(t)$ , d)  $p(t)$

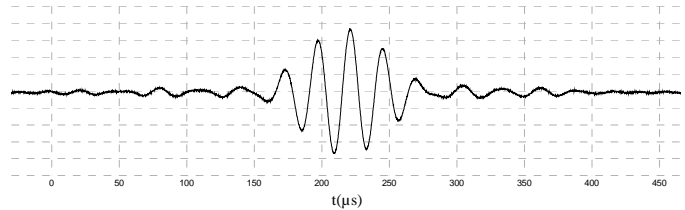


Figure 8. Detailed plot of  $M_{p\text{practical}}(t)$

As a final point, the weights  $a_k$  effectiveness is concretely tested in practice. This is illustrated on Fig. 7 and 8.

Fig. 7 compares the short pulse global system response with the one produced by the multiple pulses  $x_{MPL}(t)$  using the same set-up as shown on Fig. 2. The next figure (Fig. 8) confirms the very good match between the computed and the experiment responses,  $Mp(t)$  and  $Mp_{\text{practical}}(t)$  respectively.

Then, the two transducers were positioned face-to-face in such a way that multiple reflections would occur. With a driving signal identical to the one used previously (Fig.7), the signal received is displayed on Fig. 9. From  $x_{MPL}(t)$ , three reflections are clearly visible on this figure. In contrast, the response to  $x_{SRP}(t)$  indicates reflections and/or multi-path signals without allowing a clear identification of the reflections.

This series of experiments is concluded by the "fast repetition rate" test. Fig. 10 shows the non-overlapping system response from repetitive excitation multi-pulses  $x_{MPL}(t)$ .

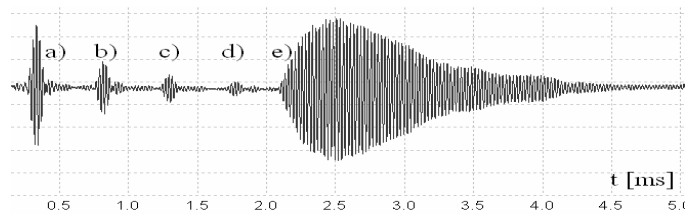


Figure 9. a) Direct wave, b) 1<sup>st</sup> reflection, c) 2<sup>nd</sup> reflection d) 3<sup>rd</sup> reflection e) Response to  $x_{SRP}(t)$

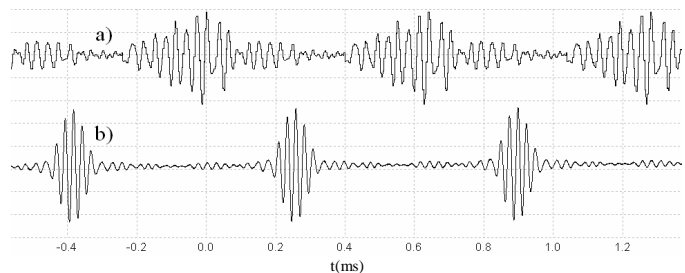


Figure 10. a) Periodic repetition of  $x_{MPL}(t)$ , b) Receiver transducer response

B. 200 kHz Piezoelectric Transducers on a PVC Tube

In this example we optimize the driving signal  $x_{MPL}(t)$  in such a way that  $Mp(t)$  has a duration of approximately 3 cycles. Fig. 11 shows the experimental arrangement where 200 kHz ultrasonic (US) transducers are glued on a PVC tube (diameter of 1cm). Figs. 12, 13 and 14 show  $p(t)$ ,  $x_{MPL}(t)$  and  $Mp(t)$  respectively. Some applications require a fast repetition rate. Therefore, we built a new driving signal with the following form

$$Mrep(t) = \sum_{k=0}^K Mp(t - k \cdot \tau) \quad (11)$$

where  $\tau = 40.8\mu s$ . Fig. 15 shows the result of this experiment.

Finally, in a multi-receivers configuration, it is easy to sequentially transmit the multi-pulses signals corresponding to each receiver; this has been confirmed by experiments conducted with four transducers.

C. Discussion

Complete series of practical tests with different kinds of transducers operating in varied conditions have confirmed the theoretical results. 100 to 300 reference pulses as well as 6 to 10 short pulses per cycles were found to be a good trade-off between effectiveness and the driving signal total duration. In the first example (i.e. 40 kHz air-transducers), the TDR duration was reduced from 60 to 4 cycles. In the second example, the TDR was also quite long (30 cycles); moreover, it had an awkward signal envelope. Even so, an OTR of three cycles was chosen and obtained in practice.

IV. CONCLUSIONS

The objective of significantly reducing the transducer to transducer time response duration has been theoretically and practically confirmed. The MMSE technique used has proven to be simultaneously robust and very effective. Many ultrasonic applications can largely benefit from this novel development; in particular, stringent transducer specifications and/or coupling requirements can be drastically relaxed.

Furthermore, situations asking for very fast repetitive excitation pulses with non-overlapping ultrasonic signal responses will also profit from this innovative solution (e.g. sampling rate reduction from pulse repetition technique).

Moreover, an adaptive solution based on the classical LMS algorithm [3] is considered as an extension of this work as well as a pulse width modulation shaping of the driving signal.

REFERENCES

- [1] Tat Hean Gan, David A. Hutchins, and Roger J. Green, "A Swept Frequency Multiplication Technique for Air-Coupled Ultrasonic NDE", IEEE Trans. Ultrason., Ferroelect., Freq. Contr., vol. 51, pp. 1271-1279, 2004
- [2] Jin-Chul Hong, Ho Sun, and Yoon Young Kim, "Waveguide Damage Detection by the Matching Pursuit Approach Employing the Dispersion-Based Chirp Functions", IEEE Trans. Ultrason., Ferroelect., Freq. Contr., vol. 53, pp. 592-605, 2006
- [3] Bernard Widrow, Samuel D. Stearns, Adaptive Signal Processing, Prentice-Hall, Inc., Englewood Cliffs, New jersey, 1985
- [4] Sophocles J. Orfanidis, Optimum Signal Processing: an Introduction, Macmillan Publishing Company, New York, 1985

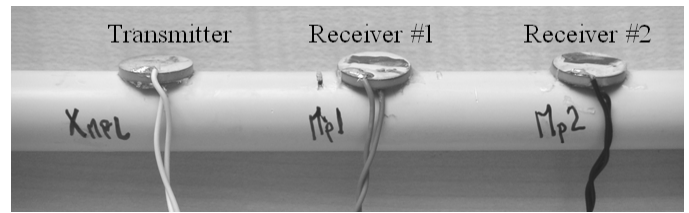


Figure 11. Experimental arrangement

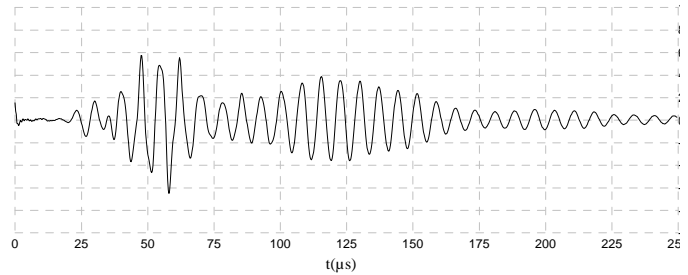


Figure 12.  $p(t)$  at receiver #1

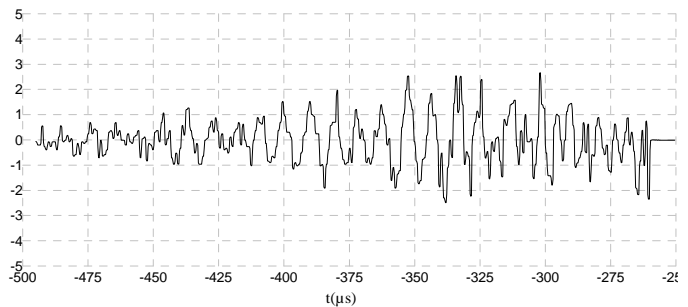


Figure 13.  $x_{MPL}(t)$  at transmitter input

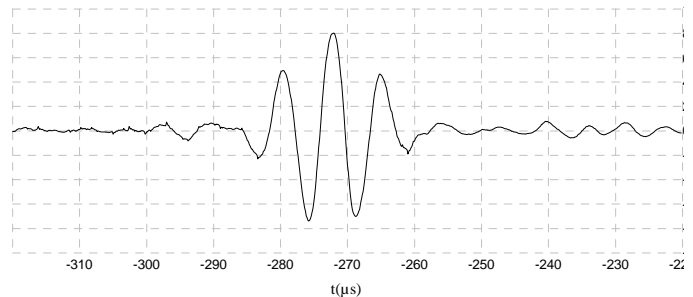


Figure 14.  $Mp_{practical}(t)$  at receiver #1

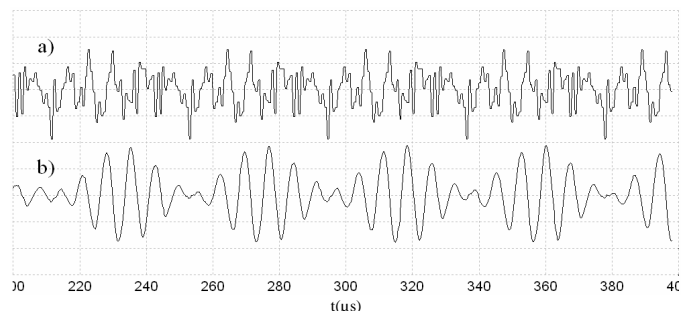


Figure 15. a) Transmitter signal, b) Signal at receiver #1